Safety Science 158 (2023) 105995

Contents lists available at ScienceDirect

Safety Science

journal homepage: www.elsevier.com/locate/safety

A Safety System based on Bluetooth Low Energy (BLE) to prevent the misuse of Personal Protection Equipment (PPE) in construction

Jesús M. Gómez-de-Gabriel [a], Juan-Antonio Fernández-Madrigal [a], María del Carmen Rey-Merchán [b], Antonio López-Arquillos [c,*]

[a] System Engineering and Automation Department, University of Málaga, Spain
[b] Consejería de Educación y Deporte. Junta de Andalucía, Spain
[c] Economics and Business Management Department, University of Málaga, Spain

ARTICLE INFO

Keywords:
Worker safety
PPE
Distance estimation
Bluetooth Low Energy (BLE)
Internet of Things (ioT)

ABSTRACT

In this paper we address the issue of safety in the use of Personal Protection Equipment (PPE) in construction, industrial, or similar sites where power tools are used. We propose a novel solution that can control *actively* the power of the tool depending on the worker–tool distance. It is based on RSSI information transmitted by BLE devices arranged in a particular rig, combined with a Bayesian distance estimator. Such an approach minimizes the required instrumentation of the workplace and also the number of configuration parameters; therefore it enables a wide range of applications. Our aim is not only to signal risky situations caused by the misuse of the PPE (either due to its bad fitting or a wrong distance to the tool), but to intervene in a fast and robust way to avoid the safety risk.

This solution is built upon previous results on the statistically sound measurement of distances and closeness in construction sites. Here, we contribute with a thorough analysis of collocating several BLE transmitters near orthogonally, which reduces interferences while avoiding the cost of more advanced technologies. We study how many transmitters are needed and what parameters are the best in the Bayesian filter for the optimal performance of the system.

Real experiments with a prototype have been conducted in a construction workshop where a person operates a miter saw. The results show how the correct use of the PPE (an earmuff equipped with the BLE transmitters) can be inferred from the distance estimation in a robust and reliable way.

1. Introduction

Occupational accidents are a worldwide cause of concern, especially in dynamic working environments, outdoor workplaces, when performing complex tasks, e.g. in the construction sector (Winge et al., 2019; López Arquillos et al., 2012; Haslam et al., 2005), or when operating power tool stations. This is pushing organizations to adapt with new strategies for safety management (Alruqi and Hallowell, 2019), such as *Prevention through Design* (PtD) (Karakhan and Gambatese, 2017; López-Arquillos and Rubio-Romero, 2015), safety training (Jeelani et al., 2018), collective prevention measures (Navon and Sacks, 2007), or *Personal Protection Equipment* (PPE) (Wong et al., 2020), which is the focus of this paper.

The misuse of PPE is associated with injuries and professional diseases such as falling from heights (Dong et al., 2017) or exposure to noise (Feder et al., 2017) —which is considered one of the most pervasive physical contaminants (Fernández et al., 2009). In general, the most frequent reasons for having problems in this sense are (Yang et al., 2020): (i) the lack of training to wear proper PPE, (ii) the reduction of productivity due to their use, (iii) being uncomfortable to wear, (iv) risk underestimation.

Although employers and managers are responsible for their workers' safety, and they are encouraged by safety recommendations to train them on the importance of PPE and to control their proper use, manual monitoring of a group of workers is very expensive and time consuming (Mneymneh et al., 2019); moreover, workers may not comply. For instance, despite the fact that in many situations the only method to reduce the exposure to noise is the use of hearing protection PPE (Kozlowski and Mlynski, 2019), workers very often decide not to wear it, or do not pay due attention to its correct fitting (Nélisse et al., 2012). In this sense, the automated management of the use of PPE is an interesting and recent field of study (Nath et al., 2020) that can play an important role in the improvement of occupational safety conditions in many industrial sectors, although its potential has not yet been fully developed (Nnaji et al., 2019).

* Corresponding author.
E-mail address: alopezarquillos@uma.es (A. López-Arquillos).

https://doi.org/10.1016/j.ssci.2022.105995
Received 12 May 2022; Received in revised form 7 October 2022; Accepted 26 October 2022
Available online 15 November 2022

In order to reduce the gap in the existing automated PPE management with respect to the pursued ideal, in this paper we propose a system that can be easily configured for a diversity of situations and provides not just detection of the correct use of the PPE, but also active risk avoidance when it is misused. For achieving both goals we use conventional BLE transmitter devices plus a statistical distance estimation method that measures the distance of the worker to the powered tool that can produce injuries. Our proposal improves not only the flexibility and cost of other solutions, but also their robustness due to the enhancement of distance estimation based on fusing RSSI signals from multiple BLE beacons collocated in the PPE (i.e., the worker). This multi-BLE device contribution avoids the use of the newest but more expensive and complicated AoA or AoD devices. In fact, our system uses RSSI signals for two different purposes, namely distance estimation and proper wearing of the PPE, which simplifies the overall design and implementation, and makes it more flexible in the sense of widening its range of applicability.

In more detail, the proposed solution consists of a single receiver attached to the powered tool, along with a microcontroller that processes the received RSSI signals from the BLE transmitters and controls the tool power source in the event of a dangerous situation—power on when the worker is not using it. On the worker side, the PPE (an earmuff in our experiments) includes a simple monitoring microcontroller that manages the set of BLE beacons transmitters to ensure an accurate and reliable distance estimation and avoid PPE misuse. Using multiple BLE transmitters in a novel composite triaxial rig maximizes the orthogonality of the transmitters, minimizing interferences; a Bayesian filtering method fuses all the beacons data statistically upon a simplified model of human displacements. All of this alleviates the signal attenuation issues and produces the best metrical estimations of the distance. Along the paper we thoroughly analyze the optimal number of BLE receivers to use in the rig and deduce the best parameters for the performance of the distance estimation filter.

The structure of the rest of the document is as follows. In Section 2 we examine previous works related to our proposal. In Section 3 the system architecture of our solution is explained in depth, as well as the real workshop scenario where our experiments have been conducted. Section 4 is devoted to a rigorous assessment of the performance of the approach and to the thorough statistical analysis that provides the best configuration parameters for the system. At the end of the section, several real experiments with our solution are described and discussed as well. The paper ends by outlining the most relevant conclusions and some future work.

2. Related works

The improvement in the design of power tool stations and the corresponding PPE instrumentation has been helping in recent years to reduce work risks. In particular, sensor-based safety management is allowing for new *smart* tools that improve safety conditions at the workplace (Asadzadeh et al., 2020). These systems can be classified according to the sensors and technologies used, as it is shown in Table 1.

The majority of these works focus on the detection of the presence of the PPE. Additionally, some of them are able to send a warning signal to the worker when a risky situation is detected, although they are not able to avoid the problem. In contrast, the proposal presented in this paper can power the tool station off if the PPE is not being used properly by the worker; thus we contribute not with a *passive* detection technology but with an *active* one that is able to act at the very source of the risk.

Some of the technologies described in Table 1 are based on the use of computer vision and machine learning. They are still passive, and require a significant computing infrastructure; besides, cameras can raise privacy issues in the workplace. Although no special devices are to be mounted onto the PPE in that case, these solutions are often impractical. To address these disadvantages the design and development of more flexible, inexpensive, robust and easy to configure systems is necessary.

A straightforward and practical approach to those issues is the estimation of the distance between the source of the risk and the worker. A number of solutions have been proposed for that purpose. For instance, the safety alert system in Teizer et al. (2010) has been designed to detect whether the equipment and the operator are in too close proximity. Similarly, a proximity alert to workers on construction sites that uses BLE (*Bluetooth Low Energy*) has recently been reported in Huang et al. (2021). Other authors propose a location-based proximity system to estimate hazard exposure (Luo et al., 2016). Since proximity detection is frequently based on limited data, it is common to include additional methods for testing that proximity (Marks and Teizer, 2013). All in all, the development of new systems for detecting the proximity of workers to occupational risks is the main topic for several authors (Wang et al., 2021; Nnaji et al., 2021; Izadi Moud et al., 2021; Rey-Merchán et al., 2020), but still, in most cases, the estimated distance is used to warn the worker to stay away from the risk source, without actively mitigating the risk. Our simpler proposal, based on multiple conventional BLE transmitters, addresses all these issues.

Estimating the distance between the worker and the risk can be based on several technologies: RF signals (e.g. RFID or Bluetooth) are particularly inexpensive and easy to deploy. RFID (*Radio Frequency Identification*) is based on wireless transponders, used mainly for presence detection, that can be implemented in a passive or active way; passive RFID transponders are easy to deploy and maintain as they do not require batteries, although they have short range, so they are not convenient in many working situations.

Methods based on Bluetooth, on the other hand, can be used for distance estimation since revision 4.0. These devices are active, but the BLE specification makes it possible to implement small transponders (the so-called BLE beacons) that periodically broadcast messages (Siekkinen et al., 2012). Bluetooth receivers can provide information about the relative attenuation of the received signal (RSSI), which can then be used to estimate distances through different methods (Wang et al., 2013; Gomez-de Gabriel et al., 2019).

More recently, the introduction of the specification 5.1 of Bluetooth in 2019 added enhanced optional localization features based on the direction-finding-capability of the Bluetooth Low Energy (BLE) standard (Suryavanshi et al., 2019). With these, a BLE receiver can estimate its relative angle to the beacon using either *Angle of Arrival* (AoA) or *Angle of Departure* (AoD) methods, using multiple antennas in either the receiver or the transmitter respectively —the transmitter needs to be upgraded to include a *Constant Tone Extension* (CTE). In this way, a single AoA receiver can estimate two angles to the transmitter with higher accuracy than the distances estimated with the RSSI (Pau et al., 2021). When using multiple synchronized and connected receivers at known locations, a tracker can even estimate the transmitter location through triangulation.

As promising and powerful as these enhanced BLE technologies are, in the end only the relative distance between the worker (using a wearable device) and the risky tool is essential for safety. More than one AoA receiver (e.g. installed in the tool) would be needed for estimating that distance with such enhanced technology, augmenting the cost and reducing the flexibility of the solution. Moreover, that would require fixed and precise locations for both the receivers and the equipment, which is not easy in working environments as dynamic as construction sites or workshops, where the number and placement of machines may change every day. Finally, the use of RSSI measurements in wearables is under variable attenuation due to the inference from the human body and the change in the polarization angle due to the worker moving around, something that these technologies do not deal with.

Table 1
Different approaches to detect the correct use of PPEs.

Sensing technology	Method	Purpose	PPE	Cite	Dataset	Precision	Freq.	Range	Require worker collab.
Vision	Deep Learning (Yolo R_CNN)	PPE use detection	Hardhat, Vest	Nath et al. (2020)	Custom (Pictor-v3)	72.3%	11 Hz	Medium	No
Vision	Deep learning (Faster R-CNN)	Hardhat use detection	Hardhat	Fang et al. (2018b)	Custom private	93.7%	5 Hz	Large	No
Vision	Deep learning benchmark dataset	Detection of hardhat use and color	Hardhat	Wu et al. (2019)	Public (GDUT-HWD)	72.3	3.2 Hz	Medium	No
Vision	Motion detection	Hardhat use detection	Hardhat	Mneymneh et al. (2019)	N/A	90.1%	18.8 Hz	Medium	No
Vision	Background subtraction	Hardhat use detection	Hardhat	Park et al. (2015)	N/A	99.6%	10 Hz	Medium	No
Vision	Background subtraction	Safety Vest use and color detection	Safety Vest	Seong et al. (2017)	Not needed	99.36%	N/A	Medium	No
Metal Detector	Sensor attached to PPE	Worker warning signal	Safety Vest	Rajendran et al. (2020)	Not needed	N/A	Continuous	Short	Yes
BLE Beacons	Relative Location, recursive Bayesian filtering	Monitoring system to detect the use of harness	Harness attached to lifeline	Gomez-de Gabriel et al. (2019)	N/A	N/A	35.36 Hz	medium	Yes
Vision	R_CNN+CNN	Safety harness detection	Harness	Fang et al. (2018a)	N/A	79.2%	N/A	Medium	No
RFID	Detection Portal and database	Control of PPE completeness	Various	Kelm et al. (2013)	N/A	100%	Once per shift	Short	Yes
RFID	Zigbee network and Cyberphysical system	Real-time PPE monitoring system	Various	Barro-Torres et al. (2012)	N/A	100%	1/600s	Short	Yes
Vision	Deep Learning (R-CNN)	System for PPE Detection	Various	Zhafran et al. (2019)	Custom private	80%	3.33 Hz	Medium	No
Embedded (optical, resistance, touch)	Wifi network and Time-stamps	PPE-Tool pair check	Various	Yang et al. (2020)	Not needed	N/A	10 Hz	Short	Yes

3. System architecture

In this section we describe the different components of the proposed system, both hardware and software (Section 3.1 and 3.2 respectively), and the working scenario where our real experiments have been carried out, as well as its instrumentation to acquire ground-truth measurements that serve for assessing the quality of the solution and find its optimal parameters (Section 3.3).

3.1. Hardware

The presented PPE system aims to provide the worker with an intelligent powered tool that can only operate when the authorized user is close enough to it and wears the appropriate personal protection equipment. The diagram of this intelligent tool approach can be seen in Fig. 1. A novel beacon rig has been designed to minimize the effects of the antenna polarization changes due to the variable orientation of the wearable as the worker moves. It has three orthogonal placeholders, denoted as X, Y and Z, for carrying BLE beacon transmitters. These beacons perform continuous (periodic) transmissions, i.e. BLE advertising. The RSSI values measured at the receiver located on the tool side are statistically filtered and fused to estimate the distance to the wearable PPE. A fourth beacon placeholder (denoted as S) holds a BLE enabled microcontroller device that advertises only while the correct use of the wearable is detected by reading a presence sensor in the PPE; if that sensor detects the PPE during a minimum safety time, the BLE transmissions are enabled until the sensor detects its absence again.

In this implementation, the beacon S attached to the PPE is composed of a BLE-enabled microcontroller (model M5StackC from M5Stack.com) and a light sensor (light dependent resistor, LDR or photoresistor) hidden inside one of the earpieces, as it can be seen in Fig. 2. It can be considered that the protective equipment is properly fitted if no light is detected. The microcontroller periodically reads the amount of light received by the LDR using an analog input to estimate the status so as to activate the BLE advertising messages only when the correct use of the PPE can be assessed.

This system can be replicated in any number of tools and users, and even manage a list of authorized users for each tool that can be dynamically and remotely updated. Absolute coordinates or locations on a map are not required; in fact, the receiver can be relocated without affecting the functionality of the approach in any way or requiring further setup. This feature is essential in dynamic environments where a centralized map setup is impractical.

3.2. Estimation method

The method for estimating the distance between the worker and the tool is based on the closeness/distance probabilistic estimator reported in Gomez-de Gabriel et al. (2019) for a single beacon. It consists of a double statistical filter: an Extended Kalman Filter (EKF) in charge of estimating the metrical distance between a BLE beacon transmitter and a receiver, and a discrete filter upon it that deduces the probability of both devices being closer than a given threshold. This approximation to the exact recursive Bayesian solution to the estimation problem, which would consist of two separate filters, is computationally very efficient and produces small errors in practice.

Here we have adapted that double estimator to be used with multiple BLE collocated beacons, which provides better performance in some measures of interest, as shown further on. More concretely, the filters in Gomez-de Gabriel et al. (2019) were devised for constant time increments between consecutive RSSI measurements, i.e., the RSSI observations come from just one beacon that can be configured with a fixed sample period, and a *non-motion model* of the transition of distances was used with constant uncertainty. Here, instead we have several beacons, that interleave their RSSI measurements from the point of view of the receiver, so it is sensible to change dynamically the

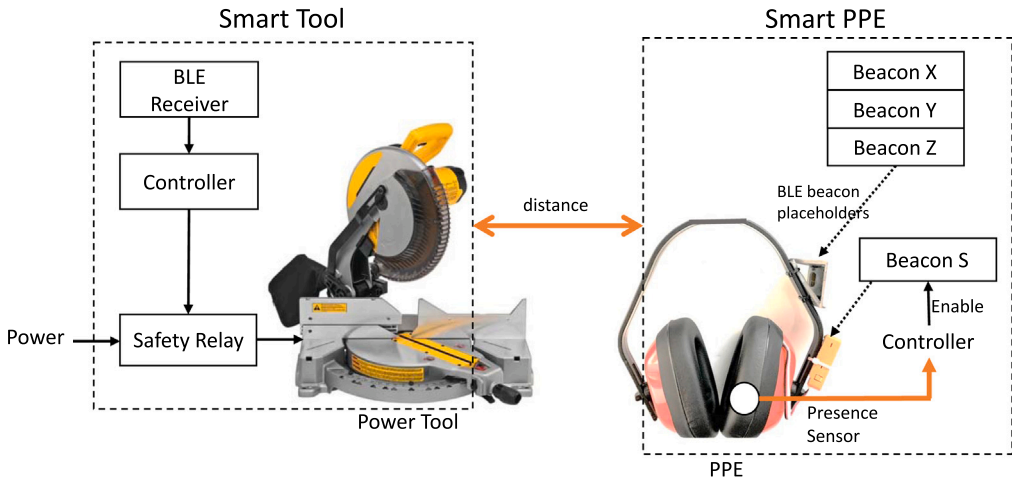

Fig. 1. Diagram of the proposed Smart Tool Approach. The PPE includes a beacon array with different antenna orientations (beacon placeholders *X*, *Y* and *Z*), while the receiver microcontroller runs the software to estimate the distance to the PPE. In addition, a user detection sensor in the PPE (beacon placeholder *S*) provides information about the correct use of the protection by the worker.

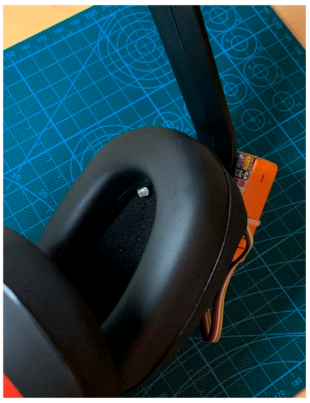

Fig. 2. Placement of the LDR sensor inside the PPE to detect its proper use.

uncertainty of each step according to the increment of time in that step (thanks to the orthogonal arrangement of transmitters in our rig, we can assume independent readings from different devices). Hence we define the transition of the transmitter–receiver distance (x_k) at step k as follows:

$$\begin{aligned} x_k &= x_{k-1} + \epsilon_k, with \epsilon_k \sim \mathcal{N}(x_k; 0, \sigma^2_{x,k}) \\ \sigma^2_{x,k} &= \left(\frac{v_{mws}\Delta_k}{2}\right)^2 \end{aligned} \quad (1)$$

where we have assumed that the worker can walk at a maximum speed of v_{mws} and the time increment in step k has been Δ_k seconds. In other words, with Eq. (1) we set that there is approximately a 95% probability of the worker having changed the distance to the receiver by $v_{mws}\Delta_k$ (uniform motion). In our experiments we use $v_{mws} = 1.5$ m/s as the approximate maximum walking speed measured for different non-disabled persons on several city streets without major obstacles during main business hours (Levine and Norenzayan, 1999). We have checked out in all our experiments that this constraint is not violated.

3.3. Working scenario

The real workshop where our field experiments have been carried out is shown in Fig. 3. There we have a miter saw (the powered tool) and a free area in front of it where the worker can move, about 5 m long. The BLE receiver is placed alongside the saw, while the worker carries the three orthogonal BLE beacons (transmitters) as explained in the previous subsections.

Before setting up our devices in a production site, we need to model the beacons behavior, i.e., to propose a theoretical distribution for the RSSI signal value that the receiver would measure from a BLE transmitter device placed at a given distance; such a model also serves to assess the performance of our filters. For building those models we require ground-truth measurements of the distance between the worker (transmitter beacons) and the saw (receiver), along with the corresponding real RSSI measurements gathered at those positions.

Due to the large uncertainty in RSSI measurements, there is no need for very high precision in the ground-truth data, so they can be obtained with simple arrangements. We have used for that an encoder connected both to the receiver and to a reel of thread; the thread is attached to the worker at the other end, so it is unrolled when going away from the reel, measuring the worker–tool distance, which can then be associated with the current RSSI value. For the encoder to measure the length of the unrolled wheel, a calibration is needed that takes into account the change in the radius of the reel as the thread unrolls, which can be done with a quadratic model.

Using this system, we have attached, in turn, 3 different BLE transmitters, referred to as '#1', '#2' and '#3', to the wearable placeholders labeled 'X', 'Y' and 'Z' in Section 3. From these physical transmitters we have gathered both RSSI and ground-truth distances over the entire range that we intend to use further on in the distance estimator filter, namely from 0 m to 5 m. In this modeling process, the worker first walked away from the saw, took a short break at the middle of the path, continued until the back of the workshop, and then returned, repeating the same pattern the other way round (see Fig. 4).

With these data, we have fitted a double exponential model with homoskedastic uncertainties (as proposed in Gomez-de Gabriel et al., 2019) to each BLE transmitter device. The exponential model provides the theoretical expectation of the RSSI values measured when the receiver and the transmitter device are at a certain distance. The fittings are shown in Fig. 5. The probability distributions for the RSSI measurements based on these models are Gaussians with $\sigma_b \simeq 5$ —otherwise, the very efficient Kalman approach would not be possible. The figures show that the Gaussian simplification is quite close to reality, but a small bias exists with respect to the real distribution of the measurements, dragging them slightly to longer distances. Also notice that, in general, the real RSSI signals are quite useful to distinguish distances that are <0.5 m approx., but not as useful if much farther than that.

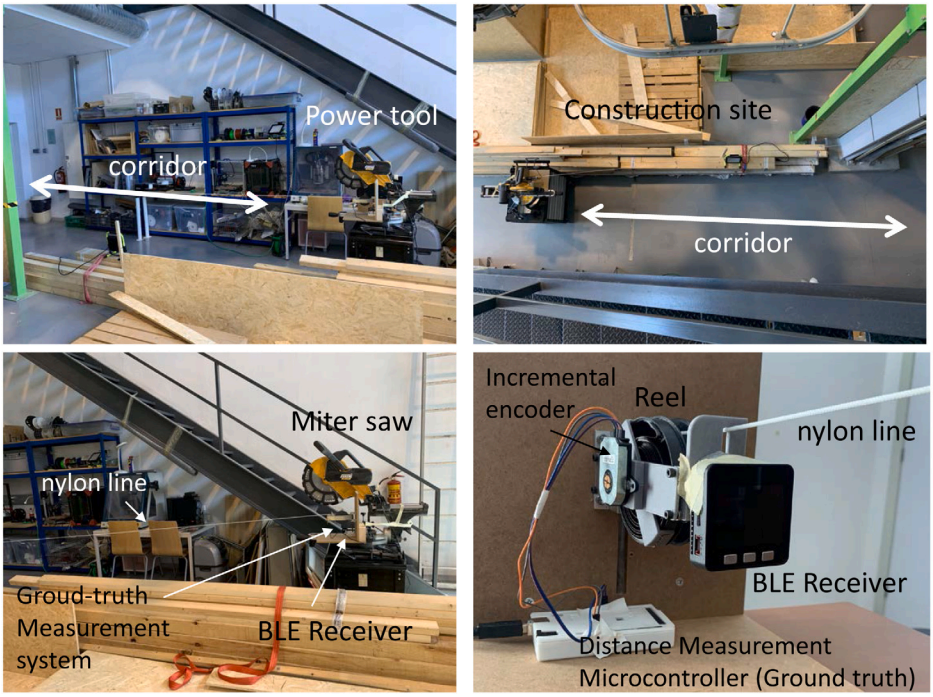

Fig. 3. Workshop environment where our solution has been validated. Top-Left: The receiver is placed to the right, where the power tool (e.g. a miter saw) is located, while the transmitter beacons move along the white line, with the worker. Top-Right: Top view of the same setting. Bottom-Left: Closer look at the saw. Bottom-Right: Detailed view of the low-cost ground-truth measurement device placed along the BLE receiver.

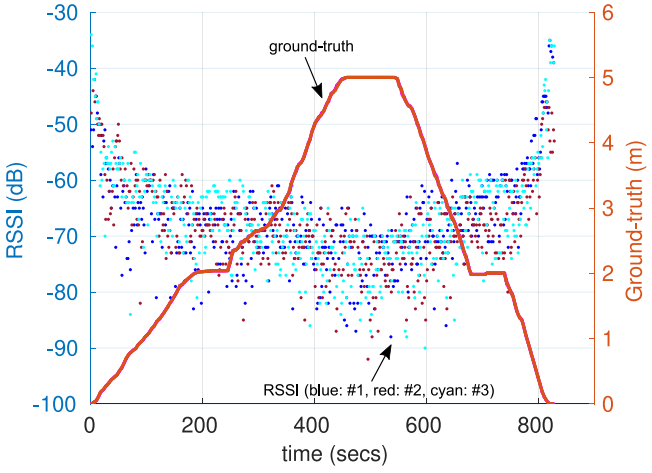

Fig. 4. Data gathered from the real workshop for creating the models of the transmitting beacons. In red, the ground-truth trajectory of the worker while walking away from and back to the saw (distance between beacons and receiver over time). In blue (#1), red (#2) and cyan (#3), the RSSI data provided by each beacon device. Approximately 100,000 RSSI and ground-truth observations were gathered per beacon, in a ~14 min walk. (For interpretation of the references to color in this figure legend, the reader is referred to the web version of this article.)

In Fig. 6-Top-Left we show the three exponential models (the theoretical expectations of the RSSI measurements) together: beacon devices #1 and #2 are more useful in short distances, while beacon #3 has greater (negative) slope in long distances and therefore may serve to estimate those distances better. These performance variations between physical devices, even those of the same model and manufacturer, are common. In Fig. 6-bottom-right we have detrended the RSSI data used for the exponential fitting in order to observe only the noise; it can be seen how the three noise distributions have a negative skewness, which confirms the longer left tail of the RSSI data compared to the theoretical normal. For alleviating this problem of the Gaussian approximation, we have decided to inflate the uncertainty of the models by using $\sigma_b = 10$, i.e., double the original one.

4. Parameter configuration and experimental results

In this section we first define some performance measures for rigorously assessing the suitability of our solution, and then deduce the best number of beacons to collocate in the wearable and the proper estimator parameters that optimize those measures (Section 4.1). In Section 4.2 we present and analyze the workshop experiments conducted with the prototype of the complete system.

4.1. Performance assessment and election of parameters

For assessing the performance of the system and also finding its best parameters (mainly the best number of transmitter beacons and the value of some EKF uncertainties), we define the following measures of interest:

- $\mathcal{M}_e$: **Accuracy or expected error**. The expected difference between the true worker–tool distance (unknown, approximated by the ground-truth) and the one estimated by our statistical filter.
- $\mathcal{M}_s$: **Precision or uncertainty in the expected error**. The standard deviation of the errors around the expected one. The smaller this measure, the more predictable will be the performance of the distance estimator under varying circumstances.
- $\mathcal{M}_l$: **Filter lag**. Any statistical filter for estimation will have a delay w.r.t. the actual dynamics of the system being estimated (the changing in worker–tool distance in our case), due to the need to collect a certain number of observations before convergence. We quantify this through the cross-correlation between the ground-truth and the estimated distance, translating the maximum of that correlation —the lag for which both signals match best— into a value in seconds.

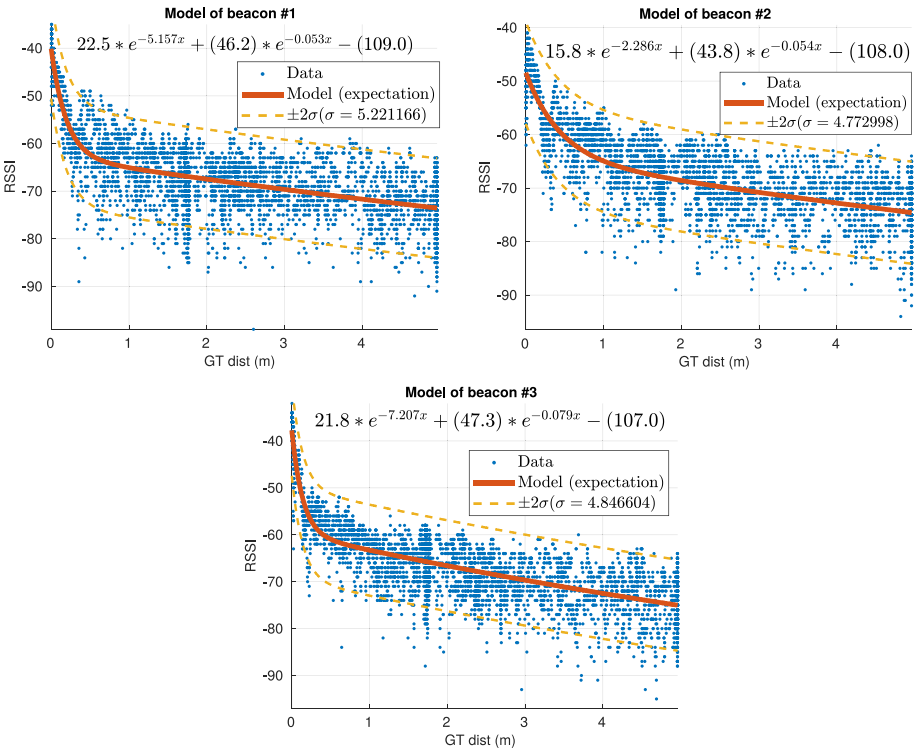

Fig. 5. Fitting of non-linear double-exponential, homoskedastic, Gaussian models to the RSSI data of the three beacons used in this work. In red, the exponential expectation; in dashed yellow, the Gaussian 2σ bands of the probability distributions centered at those expectations, all of the same variance —homoskedasticity. (For interpretation of the references to color in this figure legend, the reader is referred to the web version of this article.)

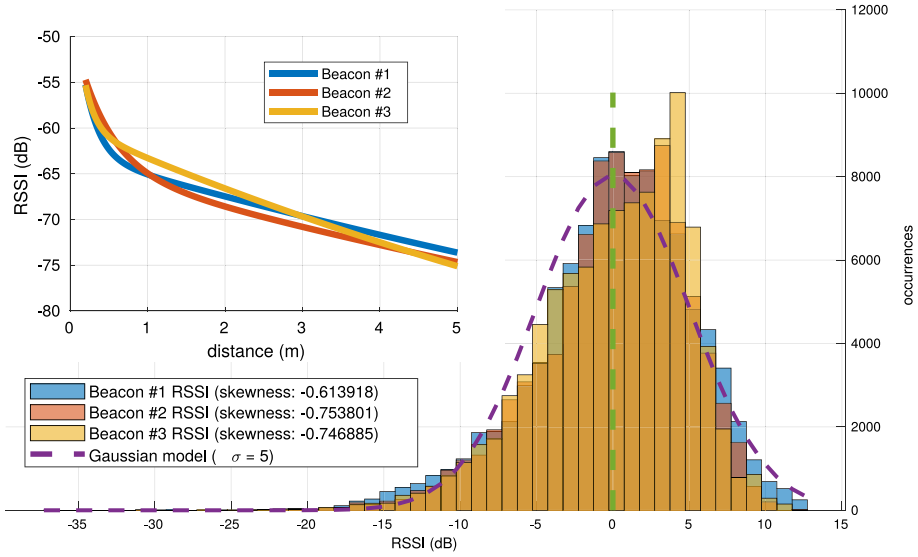

Fig. 6. Top-Left: Expectation curves provided by the exponential model of each beacon device, as a function of the beacon-receiver distance. Bottom-Right: Distribution of the RSSI noise for each beacon, once detrended with its own expectation model, compared to a $\mathcal{N}(rssi; 0, 5^2)$.

- $\mathcal{M}_a$: **All measures**. For searching for optima in the overall performance of our distance estimator, a single numeric value is needed. We use for that the weighted sum of the previous measures (each one normalized in the interval $[0, 1]$); concretely, we assign the greatest importance to the expected error of the distance estimator (weight of 0.45), then to the lag (0.35), then to the deviation of errors (0.2).

We have used these measures firstly to find the best parameters for the metrical part of the distance estimation filter, concretely the uncertainty in the RSSI likelihood (σ_b) and the one in the distance transition distribution (σ_x). In previous sections we have already set baselines for the former as $\sigma_b = 10$ (Section 3.3) and for the latter as $\sigma_x = \sqrt{\frac{v_{max}\Delta_k}{2}}$ (Section 4, Eq. (1)). In practice, inflating these uncertainties may have benefits in the filter performance: on the one hand, the actual transition distributions for the worker–tool distance will depend on the achieved speeds of the worker in each experiment, thus the previously proposed model is just a suitable starting point; on the other hand, we have already inflated the RSSI noise to cover for the observed skewness in an *ad-hoc* manner, but the theoretical

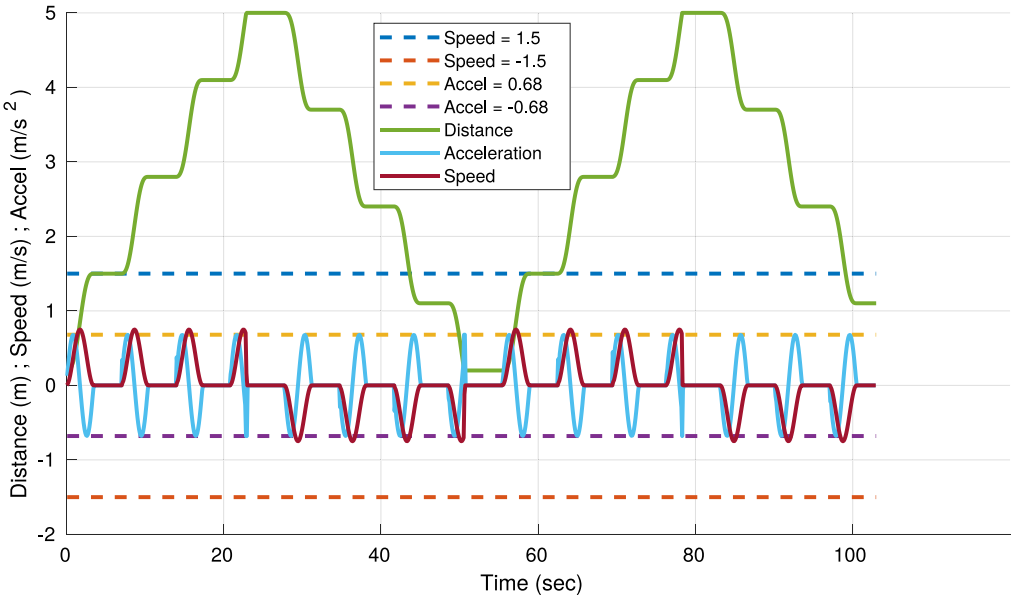

Fig. 7. Trajectory (green) of the simulated person used for the statistical search of the best parameters for our approach. The simulation considers a minimum distance of 0.2 m and a maximum of 5 m, lasts for 103 s, imposes a maximum human walking acceleration of 0.68 m/s^2 (indicated with yellow and purple dashed lines), as reported in Teknomo (2002), and forces to have certain number of walking and stopping segments. The resulting walking speeds are within the human limitation of ±1.5 m/s assumed in Section 3.2 (blue and orange dashed lines). (For interpretation of the references to color in this figure legend, the reader is referred to the web version of this article.)

independence assumption between RSSI measurements provided by different beacons is just an approximation to reality, thus we can also benefit from further tuning that uncertainty.

For this purpose we need to conduct statistically significant experiments that scan diverse combinations of transmitter beacons and of σ_b and σ_x. Gathering enough data for that is impractical in the real environment, thus we have implemented a simulated person in Matlab that carries the beacons and, while walking away from and back to the receiver —intending to reflect most common situations in working environments (see Fig. 7)—, gets both RSSI values randomly generated from the models of Section 3.3 and the true worker–tool distances. We have launched 1000 replications of that walk for each given set of beacons and combination of σ values, and then calculated the median of the 1000 tuples of the three performance measures in order to get statistically robust estimations.

As statistical experiments, these have two *factors* or independent variables: the set of transmitter beacons used in the wearable rig and the values of σ_b and σ_x. The experiments also have three *effects* or dependent variables: the three performance measures defined at the beginning of this subsection.

As for the factors, we have used 7 different rigs for the worker wearable, either with one of the available beacon devices or with tuples of three of these beacons (assuming all are placed orthogonally): { #1, #2, #3, (#1, #1, #1), (#2, #2, #2), (#3, #3, #3), (#1, #2, #3) }. For the second factor, we consider all combinations $\sigma_b = 10 \cdot \rho_b$ and $\sigma_{x,k} = \sqrt{\frac{v_{max}\Delta_k}{2}} \cdot \rho_x$, with multipliers $\rho_* \in [1,8] \subset \mathbb{N}$ (if any of these multipliers is 1, the resulting σ gets its baseline value). All in all, we have 7×8×8 = 448 different walking experiments to test, each one with 1000 replications.

In Fig. 8-Left the results of these experiments for the case of the set of beacons (#1, #2, #3) are shown. There, performance measures $\mathcal{M}_e$, $\mathcal{M}_s$, $\mathcal{M}_l$ and $\mathcal{M}_a$ are displayed separately (rows). Each color map is built upon the median of these performance measures calculated over the 1000 replications of the experiment. In these maps the diagonal patterns of the performances are clear; they come from the strong influence of the ratio σ_b/σ_x in the correction that the Kalman filter makes on its predictions to obtain estimations, namely through the Kalman gain.

Table 2
Summary of the values found for the uncertainty parameters of the distance estimator filter in order to attain their minima (best performance as of $\mathcal{M}_a$) in all the sets of beacons.

Set of beacons	ρ_b interval	ρ_x interval	$\frac{\rho_b}{\rho_x}$	Dist. to avg (0.33)
#1	(2.625, 3.375)	(7, 9)	0.371	−0.040
#2	(2.571, 3.429)	(6, 8)	0.446	−0.116
#3	(2.625, 3.375)	(7, 9)	0.375	−0.045
(#1 #1 #1)	(0.750, 1.250)	(3, 5)	0.257	+0.073
(#2 #2 #2)	(0.667, 1.333)	(2, 4)	0.296	+0.034
(#3 #3 #3)	(0.667, 1.333)	(2, 4)	0.282	+0.048
(#1 #2 #3)	(1.714, 2.286)	(6, 8)	0.284	+0.046

We show in Fig. 8-right the same medians of the performance measures, but re-grouped along the ratio ρ_b/ρ_x, the factor directly defining the ratio σ_b/σ_x. The previously shown diagonal patterns translate here into clear minima in very smooth curves.[1] Those minima correspond to the ratio of uncertainties where the filter obtains the best performance.

For the sake of space, we summarize in Table 2 the values of $\mathcal{M}_a$ for every set of transmitter devices tested for the worker wearable rig. Notice that using several identical beacons (in the sense that they are perfect replicas of the same electronic device, which is an idealization) makes more likely for the filter to not require any increment in σ_b (i.e., $\rho_b = 1$) in order to attain its best performance. In more practical cases, the ratio of multipliers is always very close to 0.33, the average of all the ratios listed in the last column of the table.

Once we have found suitable parameters for the distance estimator filter (mainly, $\rho_b/\rho_x = 0.33$), we can make the decision on how many transmitting beacons are the best choice for its performance under those parameters. To unravel this, we have employed the same measures and simulated person as before, and conducted exhaustive experiments with diverse numbers of beacons, ranging from 1 to 12, with both replicas of the same device and different devices

Fig. 9 illustrates our results for the case that $\rho_b = 2$ (hence $\rho_x = 0.66$). There you can see that the number/sets of beacons more to

[1] The experiments only sample a discrete set of values for both multipliers; we have interpolated those points through splines to get the final curves.

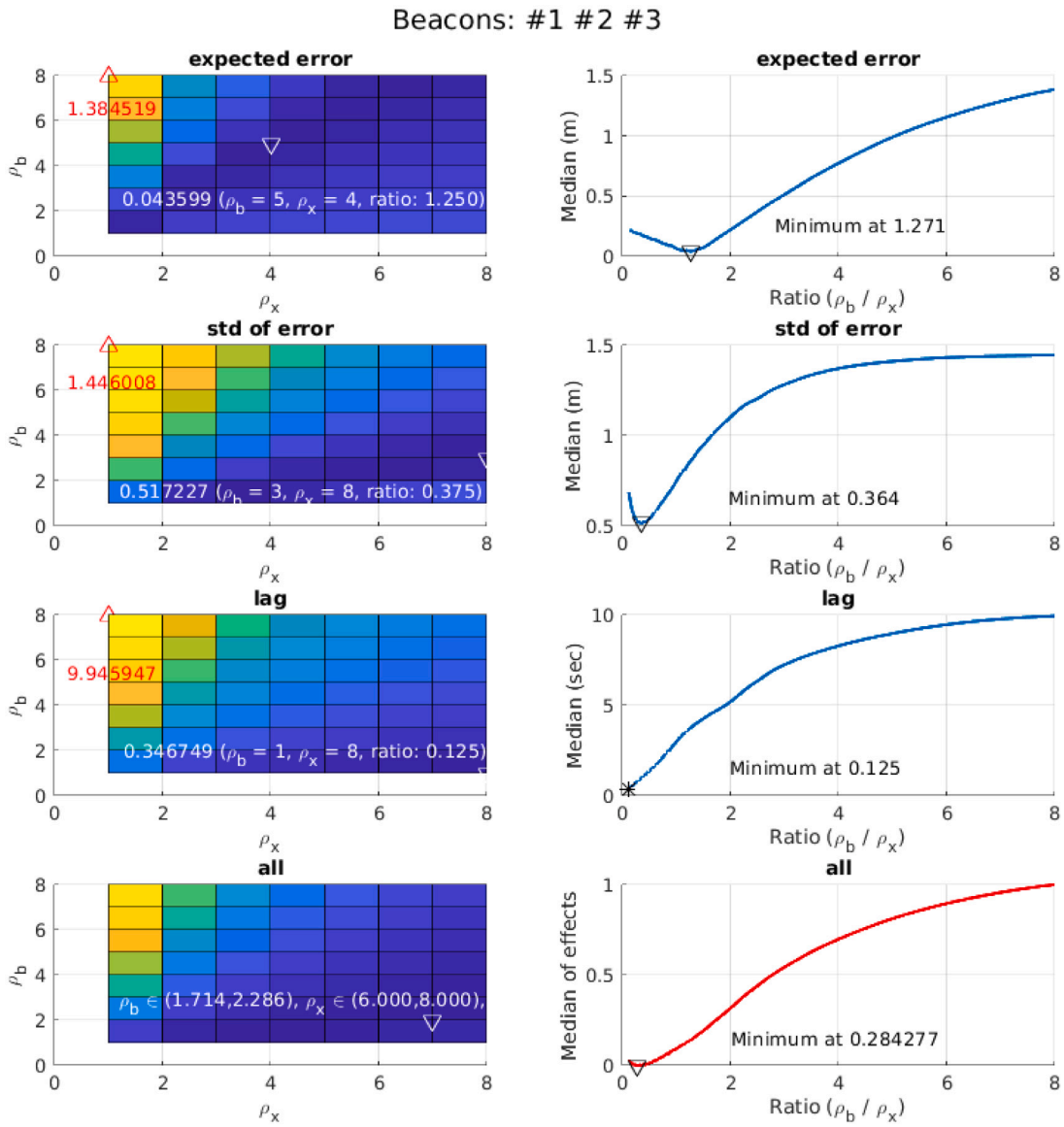

Fig. 8. Results for searching the best metrical filter parameters for a particular set of beacons, (#1, #2, #3), collocated on the simulated worker. (Left) Color map of each of the performance measures when exploring the different combinations of σ's; minima are shown in white while maxima are in red ($\mathcal{M}_e$ and $\mathcal{M}_s$: meters; $\mathcal{M}_l$: seconds). Right) Performance measure value vs. ratio of σ multipliers. (For interpretation of the references to color in this figure legend, the reader is referred to the web version of this article.)

the right of each graph are best in terms of performance; of course, if there are too many transmitter beacons in the rig, its physical implementation can be impractical or costly, and orthogonality could only be approximated.

In general, we can define, for each set of transmitters of that graph (i.e., for each location in the plane of the figure), a number that indicates its distance to the average-performance point, negative if the rig point is worse than the average, positive if it is better. We call this the *improvement distance* of that configuration. This signed number can be easily calculated from the coordinates of the rig point in the plane and those of the average point: Δ_{pos} is the position of the rig in the horizontal ordering of the graph with respect to the point of crossing with the average (i.e., the more positive Δ_{pos}, the better the overall performance), and Δ_{imp} is the improvement achieved by that rig in the overall performance with respect to the average (we multiply the vertical distance in the graph by 1000 to get an integer for Δ_{imp}; the more positive this value, the greater the improvement).

In Table 3 we collect all the improvement distances for $\rho_b \in [1, 8]$, keeping $\rho_b/\rho_x = 0.33$, in the case of $\mathcal{M}_a$. The following conclusions can be drawn:

- In general, the largest improvements are larger as we increase the number of transmitter beacons in the worker wearable (downwards in the table) and also if we use a large uncertainty for the RSSI noise (i.e., $\rho_b = 8$).
- Using a diversity of devices (#123, #123-d) is better when we use greater uncertainties for the RSSI noise or a greater number of beacons. Also notice that using all the available devices is much more realistic than having exact replicas of one device.
- Diversity in the devices (i.e., using the three of them in our case) also pays off regarding the robustness of the solution. In Table 3, the number of cases of several beacons producing worse performances than the average are: 19 (#222), 17 (#111), 12 (#333), 5 (#123), while the number of cases reporting the best performances are: 19 (#123), 9 (#111), 2 (#222), 2 (#333).

This analysis indicates that having extended the filter of Gomez-de Gabriel et al. (2019) with more than one beacon has proven to be clearly beneficial for the overall performance of the distance estimator, and suggests that, for mounting a practical rig (less than 6 beacons) and expecting a reasonable good performance in many scenarios, it

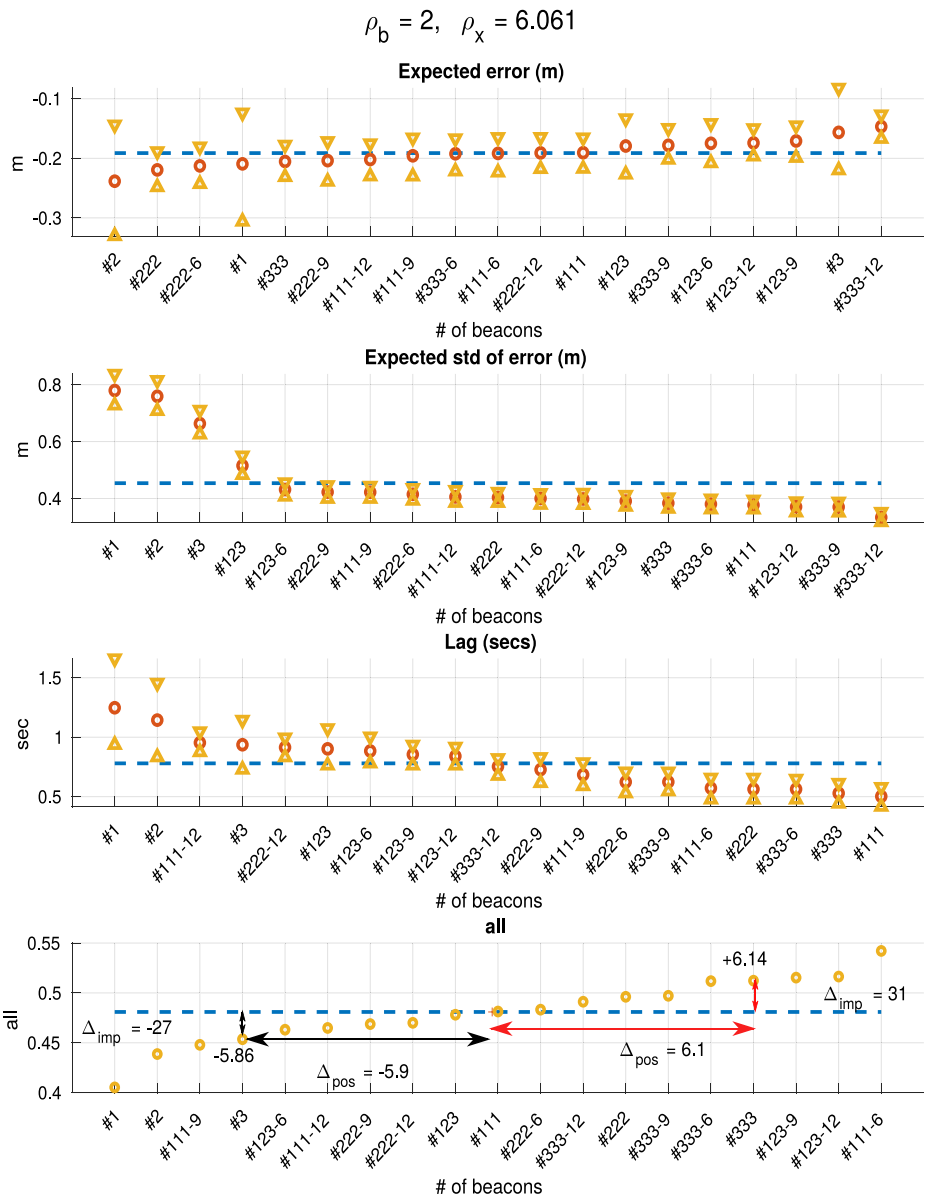

Fig. 9. Performance measures (medians + quartiles) of the worker–tool distance estimation filter when using different rigs of transmitter beacons for the worker wearable, with $\rho_b = 2$ and $\rho_b/\rho_x = 0.33$. Data are ordered from worse performance (left) to best (right). The average performance is a dashed blue line. The definitions for Δ_{pos}, Δ_{imp} and the improvement distance are illustrated in the last graph (see the main text). Legend for abscissa: **#a**: only device #a; **#abc**: 1 device #a, 1 device #b, 1 device #c; **#abc-d**: d beacons in total formed by equal amounts of devices #a, #b, and #c. (For interpretation of the references to color in this figure legend, the reader is referred to the web version of this article.)

is sensible to use 3 diverse devices and model their RSSI noise with $\rho_b \in \{4, 7\}$ (best with $\rho_b \in [4, 5]$). If cost or size is not a problem, and an approximation of orthogonality is sufficient to avoid interferences, a rig with 6 diverse beacons ((#1,#2,#3,#1,#2,#3) in our case) with $\rho_b = 8$ produces the greatest benefits in performance.

4.2. Safety experiments with the prototype

The parameters of the system found in Section 4.1, i.e., $\rho_b = 5$, $\rho_x = \rho_b/0.33$, and three different collocated BLE transmitters attached to the X, Y and Z placeholders (plus the one attached to S, in charge of indicating a correct use of the PPE), have been implemented and used for several real experiments carried out in the workshop described in Section 3.3. Here the entire software filtering system is employed, i.e., both the metrical estimation of the distance between the transmitter (worker) and the receiver (saw) and the qualitative estimation of the closeness to the saw. The latter is a discrete recursive Bayesian filter designed specifically to reflect both the closeness due to the metrical distance and the commonsense knowledge that the closeness cannot vary instantaneously; the result is a signal that varies more smoothly than the metrical distance signal alone would indicate, and therefore more suitable to implement a practically safe PPE.

Fig. 10 shows an experiment of more than 2 min where the worker changes the distance to the saw within the entire range of $[0, 5]$ m wearing the PPE correctly at all times (the relay signal and the fourth beacon transmissions are not shown). In spite of the erratic motion and the intense noise in the RSSI data, the metrical filter is able to retrieve an estimated trajectory that is very close to the true one: the expected error is ∼20 cm, a reasonable value given the noisy RSSI data, and the lag of the filter is ∼100 ms, similar to the RSSI advertising rate of one beacon. The yellow curve in Fig. 10-top-right is the probability of closeness (≤ 1 m). As it can be observed, this closeness filter provides a consistent alert indication that can be used to power the tool on or off through a relay and that does not suffer from most of the noise of

Table 3
Summary of performance improvements achieved by different rigs of transmitter beacons in the overall measure $\mathcal{M}_a$ (in red if they are worse than the average). In gray, the optimal rigs within each category of 1, 3, 6, 9 and 12 beacons).

Beacons	$\rho_b = 1$	$\rho_b = 2$	$\rho_b = 3$	$\rho_b = 4$	$\rho_b = 5$	$\rho_b = 6$	$\rho_b = 7$	$\rho_b = 8$
#1	−8.89	−8.86	−9.49	−7.66	−7.95	−0.09	0.28	−3.79
#2	−7.89	−7.86	−8.49	−4.66	−2.95	−1.09	−0.72	−4.79
#3	−6.89	−5.86	−5.49	−2.66	0.05	−3.09	−1.72	−5.79
#111	5.11	0.14	0.51	−0.66	−3.95	−11.09	−10.72	−0.79
#222	−2.89	3.14	3.51	2.34	−0.95	−6.09	−5.72	−1.79
#333	4.11	6.14	1.51	−1.66	−1.95	−5.09	−4.72	11.21
#123	0.11	−0.86	2.51	4.34	6.05	0.91	1.28	−2.79
#111–6	9.11	9.14	8.51	7.34	5.05	−7.09	−6.72	9.21
#222–6	1.11	1.14	−0.49	−3.66	−4.95	−4.09	−3.72	7.21
#333–6	−0.89	5.14	5.51	5.34	3.05	−10.09	−9.72	8.21
#123–6	−4.89	−4.86	−4.49	0.34	1.05	6.91	7.28	12.21
#111–9	−5.89	−6.86	−7.49	−6.66	−6.95	−2.09	−2.72	1.21
#222–9	6.11	−2.86	−6.49	−8.66	−8.95	−8.09	−8.72	6.21
#333–9	2.11	4.14	−2.49	−5.66	−5.95	−9.09	−7.72	0.21
#123–9	7.11	7.14	6.51	8.34	8.05	2.91	3.28	4.21
#111–12	−3.89	−3.86	−3.49	1.34	2.05	5.91	6.28	10.21
#222–12	−1.89	−1.86	−1.49	3.34	4.05	3.91	4.28	3.21
#333–12	3.11	2.14	4.51	6.34	7.05	4.91	5.28	5.21
#123–12	8.11	8.14	7.51	9.34	9.05	1.91	2.28	2.21
Best:	#111–6	#111–6	#111–6	#123–12	#123–12	#123–6	#123–6	#123-6
2nd best:	#123–12	#123–12	#123–12	#123–9	#123–9	#111–12	#111–12	#333

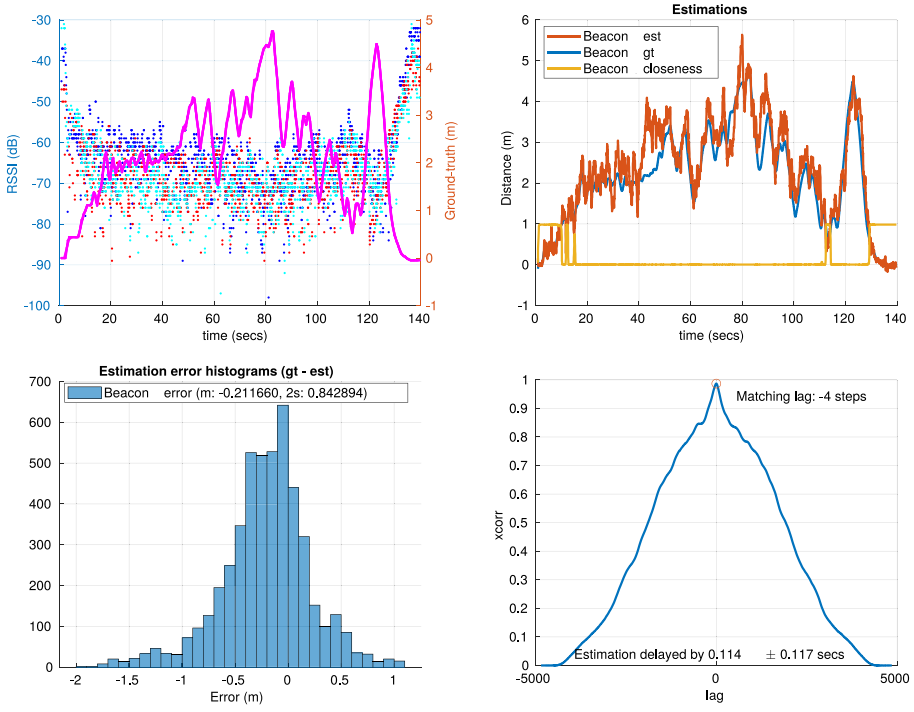

Fig. 10. Experiment with three collocated BLE transmitters while the worker walks in both directions of the workshop area and with high variance in the motion. (top-left) Ground-truth trajectory (magenta) and gathered RSSI data. top-right) Metrical distance + closeness estimation. Bottom-Left) Error in the metrical estimation. Bottom-Right) Lag of the metrical filter. (For interpretation of the references to color in this figure legend, the reader is referred to the web version of this article.)

the metrical filter. If needed, a further hysteresis filter can be added without much cost in order to eliminate the few bounces in the signal that still persist.

In the case where we use only one BLE transmitter in the worker wearable, we get the results shown in Fig. 11. The estimation is rather poor in comparison with the three-beacons rig: from best to worse, the expected errors are 27.8 cm (#2), 53 cm (#1), 62.5 cm (#3); the error deviations ($2 \cdot \sigma$) are 1.13 m (#2), 1.53 m (#3), 1.61 m (#1); and the lags are 80 ms (#1), 91 ms (#2), 438 ms (#3). Since device #2 is the best one of the three in these results, we have included in the figure the histogram of its errors in order to appreciate better the improvements achieved by the three-beacons system. Notice that, although that beacon produces similar expected error and lag compared with using the three beacon rig, its error deviation is much larger, which means that the system with only that device in the wearable is considerably less robust concerning the diversity of situations found during the experiment.

Fig. 12 shows still another experiment where the worker walks away from the saw, making short pauses from time to time, wearing the rig composed of devices #1, #2 and #3. The particularity of that experiment is that beacon #3 (the cyan points in the top-left figure) suffers from anomalies in such a way that its three channels emit with different power. In spite of that, the filter is able to recover a suitable

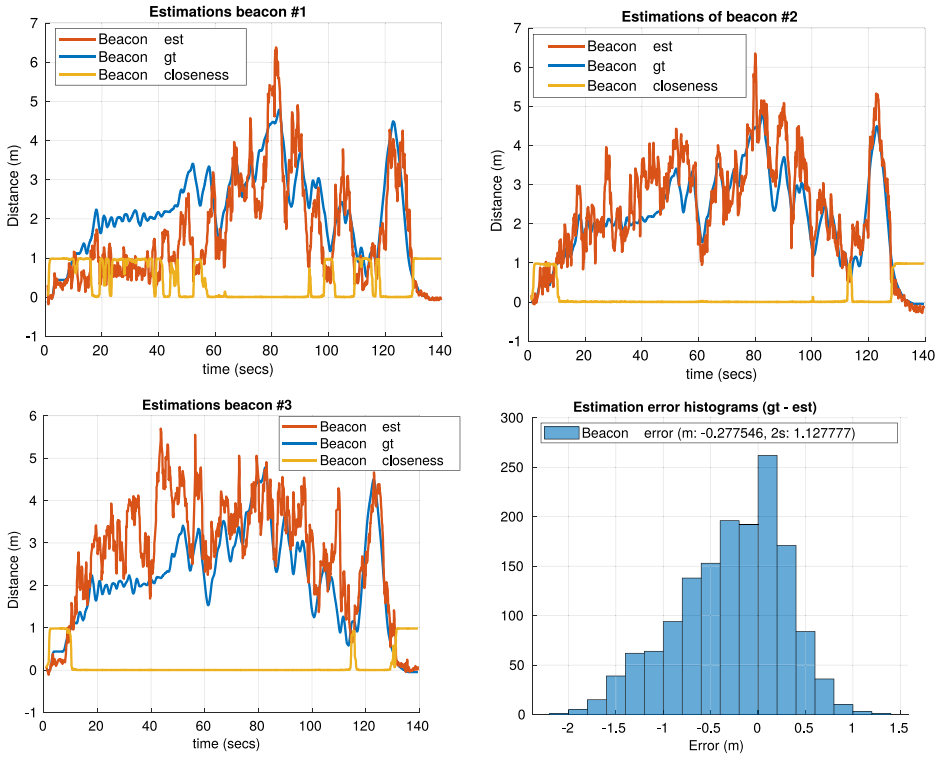

Fig. 11. The same experiment of Fig. 10 but using only the RSSI data coming from one transmitter (beacons #1, #2 and #3 in each figure, respectively). (Bottom-Right) Error histogram for the case of beacon #2.

estimated trajectory with just 12 cm of expected error and no detected lag.

If using just one device in the wearable during this experiment, we get, from best to worse, expected errors of 18.6 cm (#3), 29 cm (#2), 43 cm (#1); error deviations ($2 \cdot \sigma$) of 1.3 m (#3), 1.91 m (#2), 1.63 m (#1); and lags of 0 (#3), 0 (#2), 1.82 s (#1). The best performing one is beacon #3, but again its performance is worse than the rig of three beacons, particularly in the deviations of the error, i.e., its ability to adapt to diverse circumstances, as shown in Fig. 13.

Finally, Fig. 14 shows the effects of the worker not wearing correctly the PPE at some times. In particular, from 18 s on, the wearable is not put on during 15 s approximately; during that period, in spite of the worker being close to the tool, the tool power is kept off. The rest of the time, when the worker has the wearable correctly put on, the distance to the tool is the parameter that controls the power.

A quantitative comparison of the performance of this system with the related methods shown in Table 1 is not straightforward, as many of them employ different sensing technologies and approaches. The closest related work (Yang et al., 2020), summarized in the bottom row of that table, shares with ours the same purpose of checking the PPE-Tool presence. While Yang et al. (2020) proposes a system based on a WiFi-enabled microcontroller for both PPE and tool, the proximity detection based on timestamps and time-of-flight would require a much higher clock resolution and synchronization methods, not presented yet. The use of WiFi communications requires much more energy than BLE, preventing the use of coin-cell-powered devices in construction.

5. Conclusions and future research

In this paper we have proposed a simple cost-effective system, with high availability, for improving safety in the use of industrial powered tools. The system is composed of a set of BLE transmitters that can be attached to a wearable set and a receiver in the tool side that, endowed with proper software, estimates the metrical distance between worker and tool and provides suitable alert signals that can serve to control the power in dangerous situations (i.e., when the PPE is not properly worn and/or when the distance is beyond a given threshold).

Our practical contributions include the design of such a system, a working prototype, and a thorough statistical analysis for finding the optimal parameters for both the software and the equipment.

In this work we show that using several orthogonally collocated BLE transmitters improves robustness and overall performance with respect to just using one, without requiring more complex and costly equipment such as AoA devices. In general, the improvements are largest as we increase the number of transmitters; also, using a diversity of devices is better when these devices are noisy, and it also pays off regarding the robustness of the solution.

We have also shown that the use of an arrangement of orthogonal BLE beacons enables for an increased rate of advertising messages. An extended Kalman filter plus a discrete filter for deducing the closeness of the worker to the tool can benefit from that increased flow of data, providing a simple and efficient approximation to the problem of safety estimation in this context.

The use of an additional beacon to notify the correct use of the PPE, implemented inside a wearable microcontroller, is a very flexible solution as it allows for different local implementations using different sensors and measurements without the need to modify the RSSI-only method in the receiver, and with any number of users.

On the downside, our proposal requires a modeling phase for each transmitter device (due to the diversity of their behaviors) to be carried out before using them in production, which would increase its cost; furthermore, due to this diversity, sets of three orthogonal BLE transmitters where none of them has a good distinctive behavior at distances below the desired alert threshold should be discarded (if the threshold is below 1 m, this will occur rarely, though); also, if there are materials in the workshop that absorb radio waves (e.g., thick concrete blocks or large water cans), BLE signals can become too weak and distort the estimates; finally, protection from electromagnetic interferences caused by the power tool should be considered.

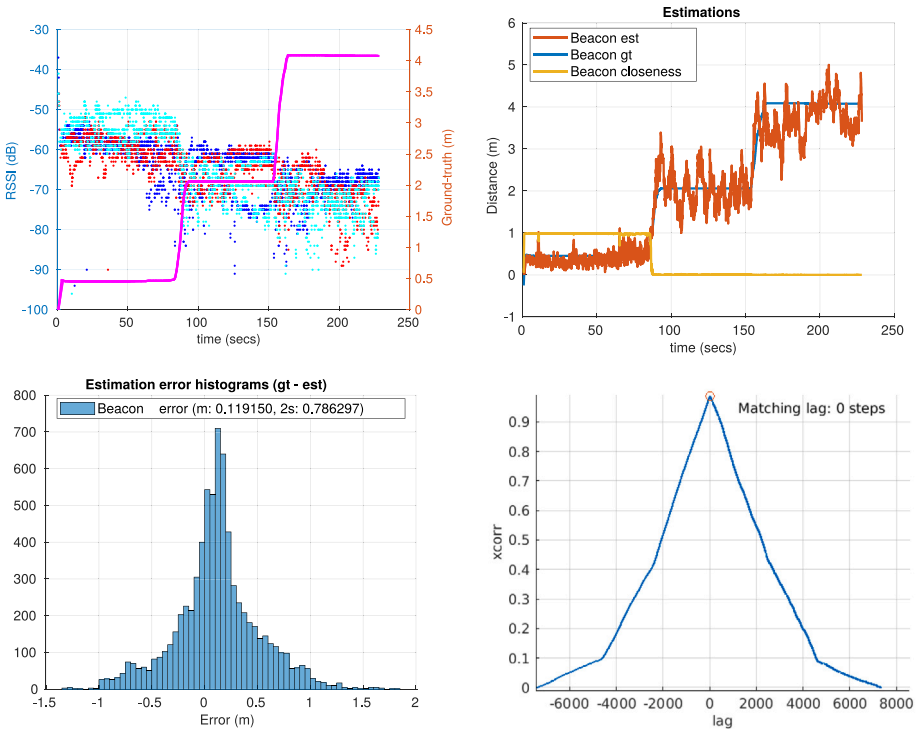

Fig. 12. Experiment with the three collocated BLE transmitters while the worker walks away from the saw, making short pauses.

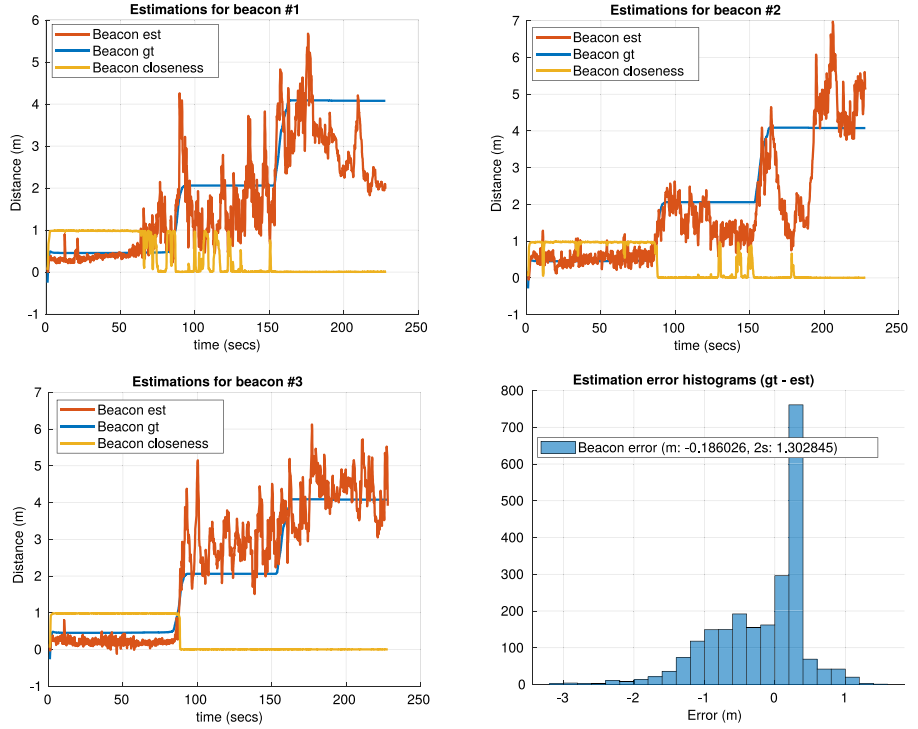

Fig. 13. The same experiment of Fig. 12 but using only the RSSI data coming from one transmitter. (Bottom-Right) Error histogram for the case of beacon #3.

In summary, after the design and testing of the system to avoid the misuse of an earmuff PPE, it can be concluded that the system is reasonably robust, cheap and easy to install. It is also quite flexible, and it can be integrated in many power tools that can be considered as a source of hazardous noise, such as a drill or miter saw, taking into account the limitations listed in the previous paragraph.

The main impact of the proposed system on construction safety is the improvement of the safety conditions through the controlled management of the workers and the risks associated with their misuse of PPE. The designed system can be easily integrated in a wide variety of dangerous machines and tools such as angle grinders, concrete mixers, pneumatic drills, etc.

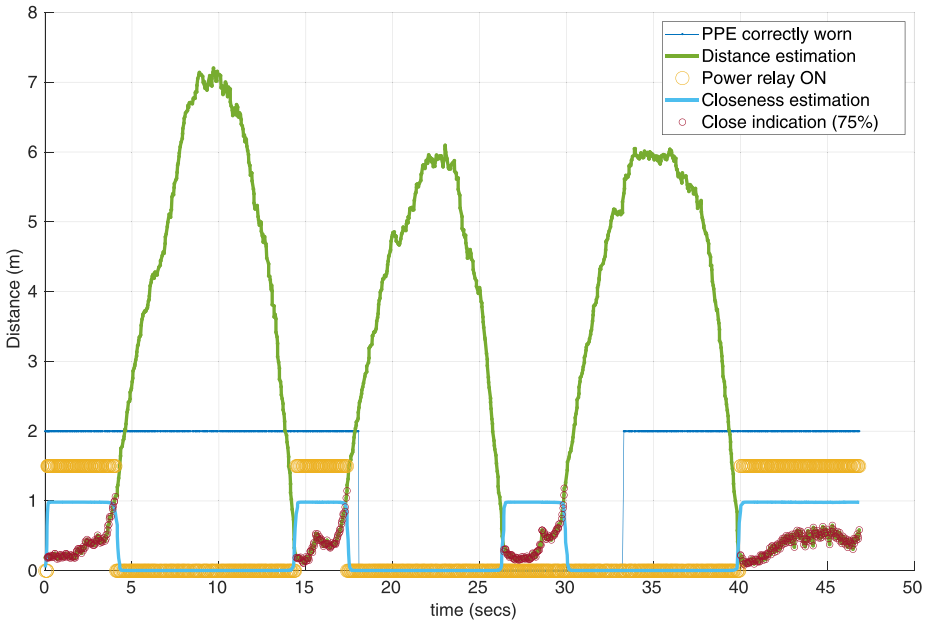

Fig. 14. Experiment with three collocated BLE transmitters while the worker walks back and forth in the environment (estimated worker–tool distance in green) but wears the PPE incorrectly from time 18,06 to time 33,22 (dark blue line). Only when the PPE is correctly worn (rest of times) and the closeness to the tool is enough (light blue line is 1) the power relay is on (yellow pulses). (For interpretation of the references to color in this figure legend, the reader is referred to the web version of this article.)

The extended use of the system in construction sites should improve the appropriate use of PPE without continuous on-site supervision of every task performed by each single worker.

Additionally, the current approach can contribute to creating a better safety culture, since the workers can perceive that the appropriate use of PPE will improve their safety and productivity.

5.1. Future research

Our ongoing works are devoted to the development of dynamic self-configuring methods for accurate distance estimation (and perhaps relative localization) that are able to monitor the misuse of PPE in relocatable equipment on the floor-plan of a factory or construction site without an a-priori map or calibration. In this sense, it is essential to conduct further research on the automatic and dynamic adaptation of the beacon models during the work, in real-time.

Also, in future research the detection of more than one PPE could be integrated in the current system. Additionally, a further analysis of the data obtained using a Fuzzy Logic System (FLS) or Artificial Intelligence could improve the safety management in the workshop according to real workers' exposure to the safety risks.

CRediT authorship contribution statement

Jesús M. Gómez-de-Gabriel: Writing – review & editing, Writing – original draft, Supervision, Resources, Project administration, Investigation, Conceptualization. **Juan-Antonio Fernández-Madrigal:** Writing – review & editing, Writing – original draft, Visualization, Validation, Supervision, Software, Methodology, Formal analysis, Data curation, Conceptualization. **María del Carmen Rey-Merchán:** Writing – review & editing, Writing – original draft, Visualization, Conceptualization. **Antonio López-Arquillos:** Writing – review & editing, Writing – original draft, Visualization, Formal analysis, Data curation, Conceptualization.

Declaration of competing interest

The authors declare that they have no known competing financial interests or personal relationships that could have appeared to influence the work reported in this paper.

Acknowledgments

This research received funding from Plan Propio-Universidad de Málaga and it is associated to the Proyecto Puente "Integración de dispositivos basados en el paradigma loT para la mejora de seguridad laboral en proyectos de contrucción (IoTcons)".

References

Alruqi, W.M., Hallowell, M.R., 2019. Critical success factors for construction safety: review and meta-analysis of safety leading indicators. J. Construct. Eng. Manage. 145 (3), 04019005.

Asadzadeh, A., Arashpour, M., Li, H., Ngo, T., Bab-Hadiashar, A., Rashidi, A., 2020. Sensor-based safety management. Autom. Constr. 113, 103128.

Barro-Torres, S., Fernández-Caramés, T.M., Pérez-Iglesias, H.J., Escudero, C.J., 2012. Real-time personal protective equipment monitoring system. Comput. Commun. 36 (1), 42–50.

Dong, X.S., Largay, J.A., Choi, S.D., Wang, X., Cain, C.T., Romano, N., 2017. Fatal falls and PFAS use in the construction industry: Findings from the NIOSH FACE reports. Accid. Anal. Prev. 102, 136–143.

Fang, W., Ding, L., Luo, H., Love, P.E., 2018a. Falls from heights: A computer vision-based approach for safety harness detection. Autom. Constr. 91, 53–61.

Fang, Q., Li, H., Luo, X., Ding, L., Luo, H., Rose, T.M., An, W., 2018b. Detecting non-hardhat-use by a deep learning method from far-field surveillance videos. Autom. Constr. 85, 1–9.

Feder, K., Michaud, D., McNamee, J., Fitzpatrick, E., Davies, H., Leroux, T., 2017. Prevalence of hazardous occupational noise exposure, hearing loss, and hearing protection usage among a representative sample of working Canadians. J. Occup. Environ. Med. 59 (1), 92.

Fernández, M.D., Quintana, S., Chavarría, N., Ballesteros, J.A., 2009. Noise exposure of workers of the construction sector. Appl. Acoust. 70 (5), 753–760.

Gomez-de Gabriel, J.M., Fernández-Madrigal, J.A., Lopez-Arquillos, A., Rubio-Romero, J.C., 2019. Monitoring harness use in construction with BLE beacons. Measurement 131, 329–340.

Haslam, R.A., Hide, S.A., Gibb, A.G., Gyi, D.E., Pavitt, T., Atkinson, S., Duff, A.R., 2005. Contributing factors in construction accidents. Applied Ergon. 36 (4), 401–415.

Huang, Y., Hammad, A., Zhu, Z., 2021. Providing proximity alerts to workers on construction sites using Bluetooth Low Energy RTLS. Autom. Constr. 132, 103928.

Izadi Moud, H., Flood, I., Zhang, X., Abbasnejad, B., Rahgozar, P., McIntyre, M., 2021. Quantitative assessment of proximity risks associated with unmanned aerial vehicles in construction. J. Manage. Eng. 37 (1), 04020095.

Jeelani, I., Han, K., Albert, A., 2018. Automating and scaling personalized safety training using eye-tracking data. Autom. Constr. 93, 63–77.

Karakhan, A.A., Gambatese, J.A., 2017. Integrating worker health and safety into sustainable design and construction: designer and constructor perspectives. J. Construct. Eng. Manage. 143 (9), 04017069.

Kelm, A., Lauß at, L., Meins-Becker, A., Platz, D., Khazaee, M.J., Costin, A.M., Helmus, M., Teizer, J., 2013. Mobile passive Radio Frequency Identification (RFID) portal for automated and rapid control of Personal Protective Equipment (PPE) on construction sites. Autom. Constr. 36, 38–52.

Kozlowski, E., Mlynski, R., 2019. Selection of earmuffs and other personal protective equipment used in combination. Int. J. Environ. Res. Public Health 16 (9), 1477.

Levine, R., Norenzayan, A., 1999. The pace of life in 31 countries. J. Cross-Cultural Psychol. 30 (2), 178–205.

López-Arquillos, A., Rubio-Romero, J.C., 2015. Proposed indicators of prevention through design in construction projects. Rev. Constr. J. Constr. 14 (2), 58–64.

López Arquillos, A., Rubio Romero, J.C., Gibb, A., 2012. Analysis of construction accidents in Spain, 2003–2008. J. Saf. Res. 43 (5–6), 381–388.

Luo, X., Li, H., Huang, T., Skitmore, M., 2016. Quantifying hazard exposure using real-time location data of construction workforce and equipment. J. Constr. Eng. Manag. 142 (8), 04016031.

Marks, E.D., Teizer, J., 2013. Method for testing proximity detection and alert technology for safe construction equipment operation. Constr. Manag. Econ. 31 (6), 636–646.

Mneymneh, B.E., Abbas, M., Khoury, H., 2019. Vision-based framework for intelligent monitoring of hardhat wearing on construction sites. J. Comput. Civ. Eng. 33 (2), 04018066.

Nath, N.D., Behzadan, A.H., Paal, S.G., 2020. Deep learning for site safety: Real-time detection of personal protective equipment. Autom. Constr. 112, 103085.

Navon, R., Sacks, R., 2007. Assessing research issues in automated project performance control (APPC). Autom. Constr. 16 (4), 474–484.

Nélisse, H., Gaudreau, M.-A., Boutin, J., Voix, J., Laville, F., 2012. Measurement of hearing protection devices performance in the workplace during full-shift working operations. Ann. Occup. Hyg. 56 (2), 221–232.

Nnaji, C., Awolusi, I., Park, J.W., Albert, A., 2021. Wearable sensing devices: towards the development of a personalized system for construction safety and health risk mitigation. Sensors 21 (3), 682.

Nnaji, C., Gambatese, J., Lee, H.W., Zhang, F., 2019. Improving construction work zone safety using technology: a systematic review of applicable technologies. J. Traffic Transp. Eng. (Engl. Ed.).

Park, M.-W., Elsafty, N., Zhu, Z., 2015. Hardhat-wearing detection for enhancing on-site safety of construction workers. J. Constr. Eng. Manag. 141 (9), 04015024.

Pau, G., Arena, F., Gebremariam, Y.E., You, I., 2021. Bluetooth 5.1: An analysis of direction finding capability for high-precision location services. Sensors 21 (11), URL: https://www.mdpi.com/1424-8220/21/11/3589.

Rajendran, S.D., Wahab, S.N., Yeap, S.P., 2020. Design of a smart safety vest incorporated with metal detector kits for enhanced personal protection. Saf. Health Work 11 (4), 537–542.

Rey-Merchán, M.d.C., Gómez-de Gabriel, J.M., Fernández-Madrigal, J.-A., López-Arquillos, A., 2020. Improving the prevention of fall from height on construction sites through the combination of technologies. Int. J. Occup. Saf. Ergon. 1–10.

Seong, H., Choi, H., Cho, H., Lee, S., Son, H., Kim, C., 2017. Vision-based safety vest detection in a construction scene. In: ISARC. Proceedings of the International Symposium on Automation and Robotics in Construction. vol. 34, IAARC Publications.

Siekkinen, M., Hiienkari, M., Nurminen, J.K., Nieminen, J., 2012. How low energy is bluetooth low energy? comparative measurements with zigbee/802.15. 4. In: 2012 IEEE Wireless Communications and Networking Conference Workshops. WCNCW, IEEE, pp. 232–237.

Suryavanshi, N.B., Viswavardhan Reddy, K., Chandrika, V.R., 2019. Direction finding capability in bluetooth 5.1 standard. In: Kumar, N., Venkatesha Prasad, R. (Eds.), Ubiquitous Communications and Network Computing. Springer International Publishing, Cham, pp. 53–65.

Teizer, J., Allread, B.S., Fullerton, C.E., Hinze, J., 2010. Autonomous pro-active real-time construction worker and equipment operator proximity safety alert system. Autom. Constr. 19 (5), 630–640.

Teknomo, K., 2002. Microscopic Pedestrian Flow Characteristics: Development of an Image Processing Data Collection and Simulation Model (Ph.D. thesis). Department of Human Social Information Sciences - Graduate School of Information Sciences - Tohoku University.

Wang, B., Wang, Y., Qiu, X., Shen, Y., 2021. BLE localization with polarization sensitive array. IEEE Wirel. Commun. Lett. 10 (5), 1014–1017. http://dx.doi.org/10.1109/LWC.2021.3055558.

Wang, Y., Yang, X., Zhao, Y., Liu, Y., Cuthbert, L., 2013. Bluetooth positioning using RSSI and triangulation methods. In: 2013 IEEE 10th Consumer Communications and Networking Conference. CCNC, IEEE, pp. 837–842.

Winge, S., Albrechtsen, E., Mostue, B.A., 2019. Causal factors and connections in construction accidents. Saf. Sci. 112, 130–141.

Wong, T.K.M., Man, S.S., Chan, A.H.S., 2020. Critical factors for the use or non-use of personal protective equipment amongst construction workers. Saf. Sci. 126, 104663.

Wu, J., Cai, N., Chen, W., Wang, H., Wang, G., 2019. Automatic detection of hardhats worn by construction personnel: A deep learning approach and benchmark dataset. Autom. Constr. 106, 102894.

Yang, X., Yu, Y., Shirowzhan, S., Li, H., et al., 2020. Automated PPE-Tool pair check system for construction safety using smart IoT. J. Build. Eng. 32, 101721.

Zhafran, F., Ningrum, E.S., Tamara, M.N., Kusumawati, E., 2019. Computer vision system based for personal protective equipment detection, by using convolutional neural network. In: 2019 International Electronics Symposium. IES, IEEE, pp. 516–521.